Tunable photoluminescence in Sb3+-doped zero-dimensional hybrid metal halides with intrinsic and extrinsic self-trapped excitons

SCHOLARONE™
Manuscripts

ROYAL SOCIETY
OF CHEMISTRY

Journal of Materials Chemistry C

Materials for optical, magnetic and electronic devices

Guidelines for Reviewers

Thank you very much for agreeing to review this manuscript for *Journal of Materials Chemistry C*.

Journal of Materials Chemistry C is a weekly journal in the materials field. The journal is interdisciplinary, publishing work of international significance on all aspects of materials chemistry related to applications in optical, magnetic and electronic devices. Articles cover the fabrication, properties and applications of materials.

Journal of Materials Chemistry C's Impact Factor is **6.641** (2018 Journal Citation Reports®)

The following manuscript has been submitted for consideration as a

FULL PAPER

For acceptance, a Full paper must report primary research that demonstrates significant **novelty and advance**, either in the chemistry used to produce materials or in the properties/ applications of the materials produced. Work submitted that is outside of these criteria will not usually be considered for publication. The materials should also be related to the theme of optical, magnetic and electronic devices.

When preparing your report, please:
- Focus on the **originality**, **importance**, **impact** and **reproducibility** of the science.
- Refer to the **journal scope and expectations**.
- **State clearly** whether you think the article should be accepted or rejected and give detailed comments (with references) both to help the Editor to make a decision on the paper and the authors to improve it.
- **Inform the Editor** if there is a conflict of interest, a significant part of the work you cannot review with confidence or if parts of the work have previously been published.
- **Provide your report rapidly** or inform the Editor if you are unable to do so.

Best regards,

Professor Peter Skabara
Editor-in-Chief
University of Glasgow, UK

Dr Sam Keltie
Executive Editor
Royal Society of Chemistry

Contact us

Please visit our reviewer hub for further details of our processes, policies and reviewer responsibilities as well as guidance on how to review, or click the links below.

What to do when you review

Reviewer responsibilities

Process & policies

Dear Reviewers,

We would like to submit our manuscript entitled "***Tunable photoluminescence in Sb³⁺-doped zero-dimensional hybrid metal halides with intrinsic and extrinsic self-trapped excitons***" authored by *Jun Zhou, Mingze Li, Maxim S. Molokeev, Jiayue Sun, Denghui Xu* and *Zhiguo Xia* for its publication in *Journal of Materials Chemistry C.*

The study on the extrinsic self-trapped excitons (STEs) caused by doping ions in metal halides become a hot issue, which can provide a feasible way for producing interesting luminescence properties. Herein, we report a novel 0D metal halide $(C_9NH_{20})_9[Pb_3Cl_{11}](ZnCl_4)_2:Sb^{3+}$, with a coexistence of intrinsic and extrinsic STEs. By regulating the Sb^{3+} concentration, the emission can be tuned from green to yellow and finally to orange, which would provide a new perspective for designing superior organic metal halide with multiple emission. We believe that this paper would be of great interest *The Journal of Materials Chemistry C* because our results are expected to have an impact on the discovery of 0D organic metal halide with tunable luminescence.

The list of key achievements which might receive the attention of the general readers are

1. We realized the tunable emission color in $(C_9NH_{20})_9[Pb_3Cl_{11}](ZnCl_4)_2:Sb^{3+}$ by adjusting the ratio of green emission from intrinsic STEs of $[Pb_3Cl_{11}]^{5-}$ clusters and red emission from extrinsic triplet STEs from $^3P_1$-$^1S_0$ transition of Sb^{3+}. Such success in 0D metal halides would provide a new perspective for designing superior organic metal halide with multiple emission.

2. By combining our dual-emitting $(C_9NH_{20})_9[Pb_3Cl_{11}](ZnCl_4)_2:0.06Sb^{3+}$, commercial $BaMgAl_{10}O_{17}:Eu^{2+}$ ($BAM:Eu^{2+}$) and NUV LED InGAN chips (λ = 395 nm), WLEDs was fabricated. The obtained CIE color coordinate is (0.345, 0.36) with color rendering index (CRI, R_a) of 71.3 and the white light correlated color temperature (*CCT*) of 4881 K, which indicate that $(C_9NH_{20})_9[Pb_3Cl_{11}](ZnCl_4)_2:0.06Sb^{3+}$ could be considered as an excellent candidate in the field of NUV WLEDs.

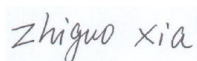Finally, in this paper the coexistence of intrinsic and extrinsic STEs in

$(C_9NH_{20})_9[Pb_3Cl_{11}](ZnCl_4)_2:Sb^{3+}$ triggers a new direction towards tuning the luminescence properties of 0D metal halides. Due to the extensive exploitation of 0D metal halides with emerging applications, the technological and scientific innovation revealed in this work, would receive the interest of numerous researchers of *Journal of Materials Chemistry C*.

We would ask your indulgence in considering our manuscript and would highly appreciate your valuable suggestions for publication. There are no relevant manuscripts by any of the authors that are submitted or in press elsewhere.

Thank you for your consideration and looking forward to hearing from you. Please do not hesitate to contact me if any additional information is needed.

Sincerely,

Zhiguo Xia

Zhiguo Xia, Professor of Materials Chemistry and Physics

School of Materials Sciences and Engineering
University of Science and Technology Beijing
No. 30 Xueyuan Road, Beijing, 100083, China
Email: xiazg@scut.edu.cn
Tel.: + 86-13810670492

ARTICLE TYPE

Tunable photoluminescence in Sb^{3+}-doped zero-dimensional hybrid metal halides with intrinsic and extrinsic self-trapped excitons

Jun Zhou[a], Mingze Li[b], Maxim S. Molokeev[c,d,e], Jiayue Sun[a], Denghui Xu[*a], and Zhiguo Xia[*b,f]

Dopants in luminescent metal halides have provided an alternative way for photoluminescence tuning towards versatile optical application. Here we report a trivalent antimony (Sb^{3+})-doped single crystalline 0D metal halide with the composition, 10 $(C_9NH_{20})_9[Pb_3Cl_{11}](ZnCl_4)_2$:$Sb^{3+}$. This compound possessed a coexistence of two emission centers including intrinsic and extrinsic self-trapped excitons (STEs), which are ascribed to $[Pb_3Cl_{11}]^{5-}$ clusters and triplet STEs formed by $^3P_1$-$^1S_0$ transition from Sb^{3+}. By regulating Sb^{3+} concentration, the emission can be 15 tuned from green to yellow and finally to orange, which would help to develop the optically pumped WLEDs with different photometric characteristics. Moreover, this dopant-induced extrinsic STEs approach presents a new direction towards tuning the luminescence properties of 0D metal halides, and may find 20 environmentally-friendly, high-performance metal halide light emitters.

1   Introduction

Organic−inorganic hybrid metal halides have attracted substantial attention for their promising application in solar cell, 25 photo-detectors, low-threshold lasers, and light emitting diodes owing to their long carrier diffusion length, adjustable band gap, and high absorption coefficients.[1-4] By selecting appropriate organic and inorganic components, three- (3D), two- (2D), one- (1D), and zero dimensional (0D) structures at the molecular level 30 can be achieved [5-7] Among these, 0D organic metal halides with broad-band emission and high exciton binding energies become hot materials due to their unprecedented optoelectronic properties, in which the metal halide molecular/cluster species are totally isolated from each other by large organic cations.[8-10]

35   To date, broad-band emission originating from metal halides is generally considered to derive from efficient self-trapped excitons (STEs). As reported, STEs are transient defects, which occurs in the excited state of a material with soft lattice and strong electron-phonon coupling, and emits photons with a large stokes 40 shift and broad spectrum.[11-14] There are normally two types of STEs in metal halides: intrinsic STEs and extrinsic STEs.[15] Most of the STEs emission in 0D metal halides reported so far is ascribed to the intrinsic STEs, such as the broad-band emission in $(C_9NH_{20})_7(PbCl_4)Pb_3Cl_{11}\cdot CH_3CN$, $(C_9NH_{20})_9(ZnCl_4)_2(Pb_3Cl_{11})$, 45 and $(C_9NH_{20})_9[Pb_3Br_{11}](MnBr_4)_2$, whose luminescence originate from intrinsic STEs formed on anionic polyhedral.[16-18] Very

recently, several articles have reported extrinsic STEs, which is due to the interaction of strong-phonon coupling and impurity-driven exciton accumulation. Chen discovered Sn-triggered 50 extrinsic STEs in 2D PEA_2PbI_4, which generates broadband extrinsic red to near infrared luminescence with a remarkable enhanced PLQYs.[19] Tang and Xia's group independently reported Cs_2SnCl_6:Sb^{3+}, which shows broad-band orange emission from extrinsic triplet self-trapped excitons.[20, 21] The results indicate that 55 it is an efficient way to dope ions into metal halides to form extrinsic STEs to produce interesting luminescence properties. However, there are few studies on the reports of the coexistence of intrinsic and extrinsic STEs in some specific 0D metal halides.

Trivalent antimony (Sb^{3+}) is an important optically active 60 luminescence ion with red broad-band emission originating from an $^3P_1$-$^1S_0$ transition.[22, 23] Up to now, several articles reported the luminescence of Sb^{3+} as matrix or activators in metal halides.[2, 20, 21, 24] However, to the best of our knowledge, the introduction of Sb^{3+} into metal halides, so as to form extrinsic STEs to realize the 65 multiple emission can benefit the formation of new emission centres and has not been reported till now. Herein, we select $(C_9NH_{20})_9[Pb_3Cl_{11}](ZnCl_4)_2$ as the starting model, by gradually replacing the Zn^{2+} in $[ZnCl_4]^{2-}$ tetrahedra with Sb^{3+} to form $(C_9NH_{20})_9[Pb_3Cl_{11}](ZnCl_4)_2$:$Sb^{3+}$. This metal halide exhibits dual-70 emission, *i.e.* simultaneously green emission from intrinsic STEs formed on $[Pb_3Cl_{11}]^{5-}$ trimer clusters and red emission from extrinsic triplet STEs formed on $^3P_1$-$^1S_0$ transition of Sb^{3+} as also found in other system.[21] With increasing Sb^{3+} concentration, the emission can be tuned from green to yellow and finally to orange. 75 The design rule established here will provide an efficient way to obtain multiple emission color by regulating the ratio of intrinsic and extrinsic STEs in 0D metal halides.

2   Experimental section

2.1   Materials and preparation

80   All the chemicals were commercially purchased and used without further purification. 1-buty-1-methylpyrrolidinium chloride ($C_9NH_{20}Cl$) (99%), lead chloride ($PbCl_2$) (99.99%), antimony chloride ($SbCl_3$) (99.99%), zinc chloride ($ZnCl_2$) (99.99%) and dimethylformamide (DMF) (99.9%), were 85 purchased from Aladdin Co. Ltd. (Shanghai, Chin). $(C_9NH_{20})_9[Pb_3Cl_{11}](ZnCl_4)_2$:$Sb^{3+}$ single crystals were synthesized as follows: $C_9NH_{20}Cl$, $PbCl_2$, ZnCl and $SbCl_3$ were dissolved in DMF under heating and continuous stirring at 323 K. The crystals

were obtained by slowly cooling the saturated solution to room temperature with the controlled cooling rate to obtain the crystals with different sizes. All chemicals were used as received from the venodrs without further purification.

2.2   Characterization methods

The diffraction patterns were collected from single crystals of $(C_9NH_{20})_9[Pb_3Cl_{11}](ZnCl_4)_2$ at 298 K using the SMART APEX II X-ray single crystal diffractometers (Bruker AXS, analytical equipment of Krasnoyarsk Center of collective use of SB RAS) equipped with a CCD-detector, graphite monochromator and Mo Kα radiation source. The absorption corrections were applied using the SADABS program. The structures were solved by the direct methods using package SHELXS and refined using the SHELXL program.[25] All hydrogen atoms were linked with C,N atoms and positioned geometrically as riding on their parent atoms with Uiso(H) = Ueq(C,N). The DIAMOND program[26] is used for the crystal structure plotting. Powder X-ray diffraction (PXRD) data of $(C_9NH_{20})_9[Pb_3Cl_{11}](ZnCl_4)_2:Sb^{3+}$ was obtained using diffractometer D8 ADVANCE (Bruker) equipped by a VANTEC detector with a Ni filter. The measurements were made using Cu Kα radiation. The structural parameters defined by single crystal analysis were used as a basic in powder pattern Rietveld refinement. The refinement was produced using TOPAS 4.2 software.[27] The morphology and particle size of the powder sample was characterized by scanning electron microscope (SEM, JEOL JSM-6510). Elemental analysis (C, H and N) of the samples was performed in a vario MACRO cube (Elementar Analysensysteme Gmbh, Germany). The room temperature excitation (PLE), room temperature emission spectra (PL) and the room-temperature decay curves were obtained using a FLSP9200 fluorescence spectrophotometer (Edinburgh Instruments Ltd., U.K.). The luminescence decay curves were obtained by the FLS920 using an nF900 flash lamp and as the excitation source. The power-dependent photoluminescence spectra were measured using the 375 nm (LE-LS-375-140TFCA, 1~140mW) laser.

3   Results and discussion

The crystal strucutre of $(C_9NH_{20})_9[Pb_3Cl_{11}](ZnCl_4)_2$ is determined by using single-crystal X-ray diffraction (SCXRD), and the unit cell corresponds to the trigonal symmetry with space group $P31c$. Detailed crystal data and structure refinement were shown in Table S1, and one can also find the crystallographic information files (CIFs) of the studied compounds $(C_9NH_{20})_9[Pb_3Cl_{11}](ZnCl_4)_2$ in the Supporting Information (SI). Fig. 1a shows the structural model and doping mechanism of as-prepared $(C_9NH_{20})_9[Pb_3Cl_{11}](ZnCl_4)_2:Sb^{3+}$, in which, the host $(C_9NH_{20})_9[Pb_3Cl_{11}](ZnCl_4)_2$ demonstrates a typical 0D structure with the individual $[ZnCl_4]^{2-}$ tetrahedra, $[Pb_3Cl_{11}]^{5-}$ trimer clusters surrounded by large organic cations $C_9NH_{20}^+$, suggesting a 0D type metal halide structure. As mentioned previously, Sb^{3+}-doped metal halides possessed interesting optical properties and were widely studied in many systems, which can bestow an intense dopant-sensitized red emission arising from the Sb^{3+}. However, to the best of our knowledge, the introduction of Sb^{3+} into metal halides, so as to form extrinsic STEs to realize the multiple emission has not been reported. Based on this, we tried to synthesize $(C_9NH_{20})_9[Pb_3Cl_{11}](ZnCl_4)_2:Sb^{3+}$ with a coexistence of

intrinsic and extrinsic STEs in order to tune the emission. Fig. S1 shows the PXRD patterns of $(C_9NH_{20})_9[Pb_3Cl_{11}](ZnCl_4)_2:Sb^{3+}$ with various Sb^{3+} concentrations. It can be found that all the diffraction peaks can be exactly indexed by the corresponding standard data for trigonal phase of $(C_9NH_{20})_9[Pb_3Cl_{11}](ZnCl_4)_2$, suggesting that doped Sb^{3+} have been successfully dissolved in the $(C_9NH_{20})_9[Pb_3Cl_{11}](ZnCl_4)_2$ host lattice. As shown in Fig. 1b, the Rietveld refinement XRD pattern of $(C_9NH_{20})_9[Pb_3Cl_{11}](ZnCl_4)_2:0.1Sb^{3+}$ can prove the succussful doping with pure phase. The unit cell volumes (V) obtained from powder pattern Rietveld refinements of $(C_9NH_{20})_9[Pb_3Cl_{11}](ZnCl_4)_2:Sb^{3+}$ are presented in Fig. 1c. The increase of V illustrates that the lattice positions of Zn^{2+} are gradually substituted by Sb^{3+} ions due to the bigger ion radii of Sb^{3+} than that of Zn^{2+}. Fig. 1d shows the SEM images of $(C_9NH_{20})_9[Pb_3Cl_{11}](ZnCl_4)_2:Sb^{3+}$ (~ 5 μm), and the elemental mapping images in Fig. 1e-h indicated that Pb, Cl, Zn and Sb are homogeneously distributed within the particles.
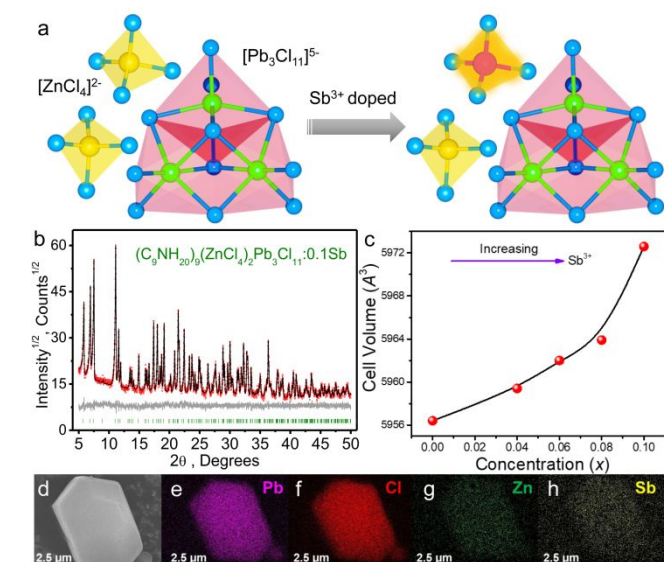

Fig. 1. Diagram of structural model and doping mechanism of $(C_9NH_{20})_9[Pb_3Cl_{11}](ZnCl_4)_2:Sb^{3+}$. (a) Schematic illustration of the synthesis process of Sb^{3+} doped $(C_9NH_{20})_9[Pb_3Cl_{11}](ZnCl_4)_2$ crystals. (b) PXRD profile for Rietveld refinement of $(C_9NH_{20})_9[Pb_3Cl_{11}](ZnCl_4)_2:0.1Sb^{3+}$. (c) Dependence of unit cell volumes from powder pattern Rietveld refinement on different Sb^{3+} doping concentrations. (d-h) SEM and elemental mapping images of Pb, Cl, Zn and Sb for the selected $(C_9NH_{20})_9[Pb_3Cl_{11}](ZnCl_4)_2$ particle.

Optical properties of Sb^{3+}-doped $(C_9NH_{20})_9[Pb_3Cl_{11}](ZnCl_4)_2$ were fully characterized as discussed below. Fig. 2a shows the images of the pristine and Sb-doped $(C_9NH_{20})_9[Pb_3Cl_{11}](ZnCl_4)_2$ under 365 nm excitation at room temperature. $(C_9NH_{20})_9[Pb_3Cl_{11}](ZnCl_4)_2$ displays highly bright green emission, and the emission colours of the samples can be tuned from green to yellow and finally to orange with increasing Sb^{3+} concentration. Sb^{3+} belongs to $5S^2$ outer electronic configurations and the splitting of the energy levels can be expressed as shown in Fig. 2b. The ground state of s^2 ion is $^1S_0$, whereas the excited state can split into four energy levels: $^3P_0$, $^3P_1$, $^3P_2$ and $^1P_1$. Based on the transition rule, the transitions of $^1S_0$-$^3P_2$ and $^1S_0$-$^3P_0$ are completely forbidden, while the transition of $^1S_0$-$^1P_1$ is allowed and $^1S_0$-$^3P_1$ transition is partially allowed owing to a spin-orbit

coupling for heavy atoms. The photoluminescence within the visible light region is possibly caused by the $^3P_1$-$^1S_0$ transition.[21] The photoluminescence spectra of $(C_9NH_{20})_9[Pb_3Cl_{11}](ZnCl_4)_2$:$Sb^{3+}$ at room temperature are shown in Fig. 2c. Upon excitation at 330 nm, $(C_9NH_{20})_9[Pb_3Cl_{11}](ZnCl_4)_2$ exhibits a bright green emission peaked at 512 nm with a Stokes shift of 182 nm and a full width at half maximum (FWHM) of 61 nm, corresponding to intrinsic STEs of $[Pb_3Cl_{11}]^{5-}$ clusters.[17] When doping Sb^{3+} ions, a broad emission band cantered at 630 nm with a large Stokes shift of 265 nm, is observed in the PL spectra. The emission of 630 nm is due to the allowed transition ($^3P_1$ to $^1S_0$) of Sb^{3+} ions, while the large Stokes shift is due to that outermost S-P electron orbital transition of Sb^{3+} was highly sensitive to the crystal field the distortion of Sb-Cl polyhedron.[28, 29] With the increase of Sb^{3+} concentration, $(C_9NH_{20})_9[Pb_3Cl_{11}](ZnCl_4)_2$:$Sb^{3+}$ exhibited similar PLE spectra, while the ratio of red emission band intensity to green emission band intensity increases. Hence, the emission colour of the samples gradually is changed from green to yellow and finally to

orange, which is consistent with the digital images in Fig. 2a. It is worth noting that there is no energy transfer between $[Pb_3Cl_{11}]^{5-}$ clusters and Sb^{3+} here, but a mixture luminescence from different polyhedrons. The reasons are explained as follows: 1. Compared with the PL spectrum of $(C_9NH_{20})_9[Pb_3Cl_{11}](ZnCl_4)_2$ and PLE spectrum of $(C_9NH_{20})_9[Pb_3Cl_{11}](ZnCl_4)_2$:$Sb^{3+}$, there is little overlap between them; 2. The PLE spectra between $(C_9NH_{20})_9[Pb_3Cl_{11}](ZnCl_4)_2$ and $(C_9NH_{20})_9[Pb_3Cl_{11}](ZnCl_4)_2$:$Sb^{3+}$ are quite different, suggesting that $(C_9NH_{20})_9[Pb_3Cl_{11}](ZnCl_4)_2$ does act as a sensitizer.[30] In order to gain an insight into the luminous mechanism of multiple emission centers, room-temperature decay curves of these $(C_9NH_{20})_9[Pb_3Cl_{11}](ZnCl_4)_2$:$Sb^{3+}$ were carried out (Fig. 2d). The emission decay profiles collected at 512 nm of the pristine and 630 nm of Sb-doped $(C_9NH_{20})_9[Pb_3Cl_{11}](ZnCl_4)_2$ are from the contribution of the intrinsic STEs of $[Pb_3Cl_{11}]^{5-}$ clusters and extrinsic triplet STEs of from $^3P_1$-$^1S_0$ transition of Sb^{3+}, respectively. All luminescence decay curves can be well fitted with a single order exponential equation:[31]
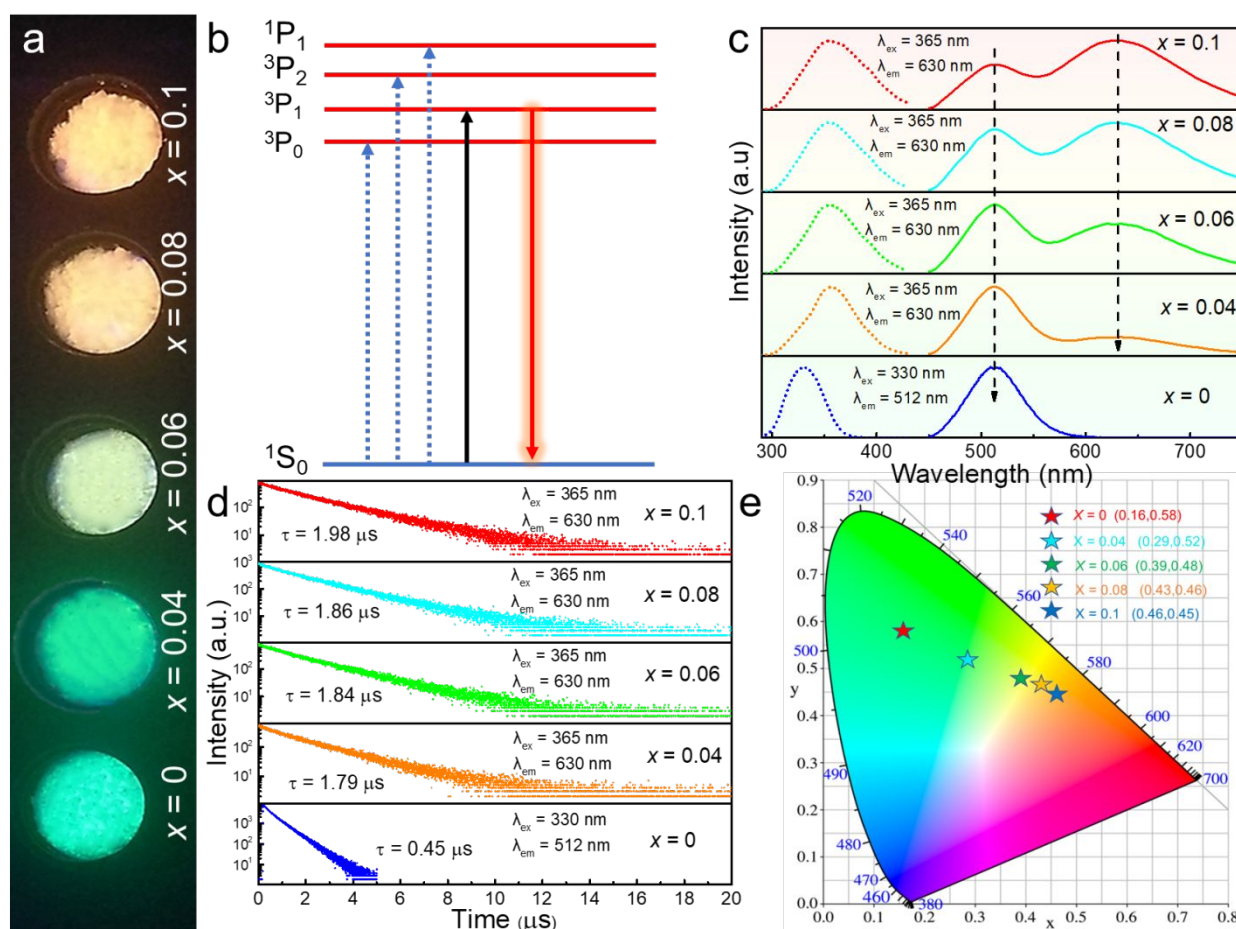
Fig. 2. (a) Digital images of some selected $(C_9NH_{20})_9[Pb_3Cl_{11}](ZnCl_4)_2$:$Sb^{3+}$ samples under 365 nm UV lamp. (b) Schematic diagram of luminescence process for Sb^{3+} in $(C_9NH_{20})_9[Pb_3Cl_{11}](ZnCl_4)_2$:$Sb^{3+}$. (c) Room-temperature PL and PLE spectra of $(C_9NH_{20})_9[Pb_3Cl_{11}](ZnCl_4)_2$:$Sb^{3+}$ under different Sb^{3+} concentrations excited at 365 nm and 330 nm. (d) Room-temperature photoluminescence decay curves of $(C_9NH_{20})_9[Pb_3Cl_{11}](ZnCl_4)_2$:$Sb^{3+}$ depending on the emission wavelengths at 365 nm and 330 nm excitation. (e) CIE chromaticity diagram of $(C_9NH_{20})_9[Pb_3Cl_{11}](ZnCl_4)_2$:$Sb^{3+}$ excited at 330 nm and 365 nm.

$$I(t) = A\exp(-t/\tau) \tag{1}$$

where I is the luminescence intensity, t is the time after excitation, A is a constant and τ is the radiative decay time. Based on Eq.(1),

the effective decay time of green band was calculated to be 0.45 µs, while that of red band with different Sb^{3+} contents were 1.79-1.98 µs. Among them, the long lifetime of microsecond is

consistent with the previous reports in Sb-doped metal halides.[2, 21, 24] Moreover, the lifetime values of Sb^{3+} tend to increase with the increasing content of Sb^{3+} ions, demonstrating that radiative transition is enhanced in $(C_9NH_{20})_9[Pb_3Cl_{11}](ZnCl_4)_2:Sb^{3+}$. Fig. 2e shows the corresponding CIE coordinates of the emissions from the pristine and Sb-doped $(C_9NH_{20})_9[Pb_3Cl_{11}](ZnCl_4)_2$. By combining the green band from the $[Pb_3Cl_{11}]^{5-}$ clusters and red band from $^3P_1$-$^1S_0$ transition of Sb^{3+}, the emission color tone can be tuned from green (0.16, 0.58) to yellow (0.39, 0.48) and finally to orange (0.46, 0.45). The wide colour tunability of these $(C_9NH_{20})_9[Pb_3Cl_{11}](ZnCl_4)_2:Sb^{3+}$ would help to develop the optically pumped WLEDs with tunable photometric characteristics for different optical applications.

STEs emission acts as a typical mechanism that can explain the large Stokes shift of many luminescent metal halide materials.[15] Therefore, we speculate that the luminescence at 630 nm also originates from STEs, just like that at 512 nm. In order to prove it, the variation of the emission intensities excited at 375 nm as a function of the excitation power density were tested and shown in Fig. 3a. The PL intensities at 630 nm of $(C_9NH_{20})_9[Pb_3Cl_{11}](ZnCl_4)_2:0.06Sb^{3+}$ increase linearly with the excitation power density from 0 to 1500 mW/cm^2 at 300 K, which further verify the origins of the triplet STEs for the 630 nm emission centers. Therefore, the excited state processes for this 0D organic metal halide hybrid $(C_9NH_{20})_9[Pb_3Cl_{11}](ZnCl_4)_2:Sb^{3+}$ can be depicted as shown in Fig. 3b. Upon 330 nm (3.76 eV) excitation, lattice distortion in $[Pb_3Cl_{11}]^{5-}$ clusters caused by the strong electron-phonon interactions will prompt the ultrafast formation of STEs, resulting in green emission. While upon 365 nm (3.40 eV) excitation, the electrons of Sb^{3+} in the ground states are excited, then undergo the ultrafast excited-state reorganization from the high-energy excited states to the triplet STEs following $^3P_1$-$^1S_0$, and exhibit Stokes-shifted red broadband emission. It is worth mentioning that the STEs of $[Pb_3Cl_{11}]^{5-}$ clusters is the intrinsic emission center, while the triplet STEs from $^3P_1$-$^1S_0$ transition of Sb^{3+} corresponds to extrinsic one by doping.
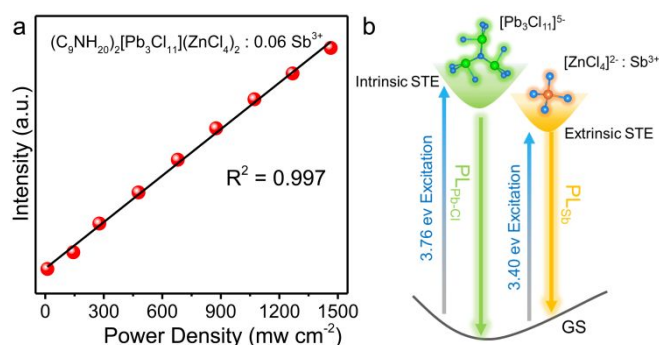
Fig. 3. (a) Dependence of emission intensity at 630 nm in $(C_9NH_{20})_9[Pb_3Cl_{11}](ZnCl_4)_2:0.06Sb^{3+}$ on excitation intensity (0 − 1500 mW/cm^2) at 300 K and a linear fit (λ_{ex} = 375 nm). (b) Diagram of luminescence processes in $(C_9NH_{20})_9[Pb_3Cl_{11}](ZnCl_4)_2:Sb^{3+}$ at room temperature.

As a typical example, the green/red dual-emitting $(C_9NH_{20})_9[Pb_3Cl_{11}](ZnCl_4)_2:0.06Sb^{3+}$ has been used in optically pumped LEDs. We fabricated WLEDs by combining our $(C_9NH_{20})_9[Pb_3Cl_{11}](ZnCl_4)_2:0.06Sb^{3+}$ sample, the commercial blue phosphor $BaMgAl_{10}O_{17}:Eu^{2+}$ (BAM:Eu^{2+}) and NUV LED

InGAN chips (λ = 395 nm). Fig. 4a shows the PL spectra of the WLED device under a current of 20 mA, and the inset shows the photographs of the fabricated WLED device. The obtained result reveals that the CIE color coordinate is (0.345, 0.360) with color rendering index (CRI, R_a) of 71.3 and the white light correlated color temperature (*CCT*) of 4881 K (Fig. 4b). The above results indicate that $(C_9NH_{20})_9[Pb_3Cl_{11}](ZnCl_4)_2:0.06Sb^{3+}$ could be considered as an excellent candidate in the field of NUV WLEDs.
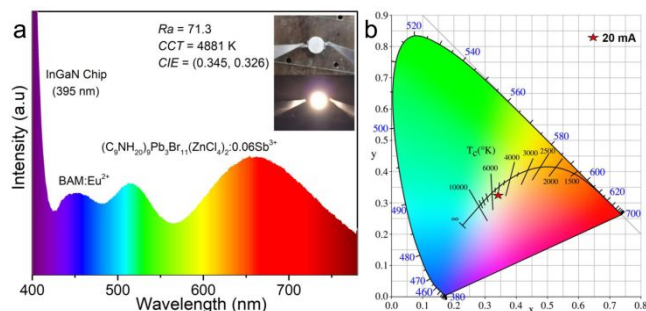
Fig. 4. (a) PL spectra of WLED fabricated by our phosphor $(C_9NH_{20})_9[Pb_3Cl_{11}](ZnCl_4)_2:0.06Sb^{3+}$, and commercial blue phosphor BAM:Eu^{2+}on a 395 nm InGAN chip at 20 mA drive current. (b) CIE chromaticity diagram of $(C_9NH_{20})_9[Pb_3Cl_{11}](ZnCl_4)_2:0.06Sb^{3+}$ of the fabricated WLED.

4   Conclusion

In summary, Sb dopant triggers the occurrence of extrinsic STEs in $(C_9NH_{20})_9[Pb_3Cl_{11}](ZnCl_4)_2$ except for the intrinsic emission center originating from STEs of $[Pb_3Cl_{11}]^{5-}$ clusters, which enrich the design principle in luminescent metal halides to realize the tunable emission colors. By adjusting the doping concentration of Sb^{3+}, the ratio of green emission from intrinsic STEs of $[Pb_3Cl_{11}]^{5-}$ clusters and red emission from extrinsic triplet STEs from $^3P_1$-$^1S_0$ transition of Sb^{3+} is also adjusted, so that the luminescent color of the halide changes remarkably from green to yellow and finally to orange. Such success in 0D metal halides would provide a new perspective for designing superior organic metal halide with multiple emission, which would also allow for the development of optically pumped WLEDs with different photometric properties for various applications.

Supporting Information

The crystallographic information file (CIF) of $(C_9NH_{20})_9[Pb_3Cl_{11}](ZnCl_4)_2$ is presented. This material is available free of charge via the Internet at http://pubs.acs.org.

Acknowledgements

Notes and references

a School of Science, Beijing Technology and Business University, Beijing 100048, P. R. China

*xudh@btbu.edu.cn (D. Xu)

b The Beijing Municipal Key Laboratory of New Energy Materials and Technologies, School of Materials Sciences and Engineering, University of Science and Technology Beijing, Beijing 100083, China

c Laboratory of Crystal Physics, Kirensky Institute of Physics, SB RAS, Krasnoyarsk 660036, Russia

d Siberian Federal University, Krasnoyarsk, 660041, Russia

e Department of Physics, Far Eastern State Transport University, Khabarovsk, 680021, Russia

f State Key Laboratory of Luminescent Materials and Devices and Institute of Optical Communication Materials, South China University of Technology, Guangzhou, 510641, China

* E-mail: xiazg@scut.edu.cn (Z. Xia)

Notes and references

1. P. J. Guo, C. C. Stoumpos, L. L. Mao, S. Sadasivam, J. B. Ketterson, P. Darancet, M. G. Kanatzidis and R. D. Schaller, *Nat. Commun.*, 2018, **9**, 2019.

2. Z. Y. Li, Y. Li, P. Liang, T. L. Zhou, L. Wang and R. J. Xie, *Chem. Mater.*, 2019, **31**, 9363-9371.

3. S. Yakunin, B. M. Benin, Y. Shynkarenko, O. Nazarenko, M. I. Bodnarchuk, D. N. Dirin, C. Hofer, S. Cattaneo and M. V. Kovalenko, *Nat. Mater.*, 2019, **18**, 846-852.

4. Z. P. Wang, Z. Z. Zhang, L. Q. Tao, N. N. Shen, B. Hu, L. K. Gong, J. R. Li, X. P. Chen and X. Y. Huang, *Angew. Chem.* , 2019, **58**, 9974-9978.

5. L. L. Mao, Y. L. Wu, C. C. Stoumpos, B. Traore, C. Katan, J. Even, M. R. Wasielewski and M. G. Kanatzidis, *J. Am. Chem. Soc.*, 2017, **139**, 11956-11963.

6. H. R. Lin, C. K. Zhou, Y. Tian, T. Siegrist and B. W. Ma, *ACS Energy. Letters.*, 2017, **3**, 54-62.

7. Y. Q. Liao, H. F. Liu, W. J. Zhou, D. W. Yang, Y. Q. Shang, Z. F. Shi, B. H. Li, X. Y. Jiang, L. J. Zhang, L. N. Quan, R. Quintero-Bermudez, B. R. Sutherland, Q. X. Mi, E. H. Sargent and Z. J. Ning, *J. Am. Chem. Soc.*, 2017, **139**, 6693-6699.

8. G. Giorgi and K. Yamashita, *J. Phys. Chem. Lett.*, 2016, **7**, 888-899.

9. S. Brochard-Garnier, M. Paris, R. Génois, Q. Han, Y. Liu, F. Massuyeau and R. J. A. F. M. Gautier, *Adv. Funct. Mater.* , 2019, **29**, 1806728.

10. V. Morad, Y. Shynkarenko, S. Yakunin, A. Brumberg, R. D. Schaller and M. V. Kovalenko, *J. Am. Chem. Soc.*, 2019, **141**, 9764-9768.

11. T. Hu, M. D. Smith, E. R. Dohner, M. J. Sher, X. X. Wu, M. T. Trinh, A. Fisher, J. Corbett, X. Y. Zhu, H. I. Karunadasa and A. M. Lindenberg, *J. Phys. Chem. Lett.*, 2016, **7**, 2258-2263.

12. M. D. Smith, A. Jaffe, E. R. Dohner, A. M. Lindenberg and H. I. Karunadasa, *Chem. Sci.*, 2017, **8**, 4497-4504.

13. M. D. Smith and H. I. Karunadasa, *Acc. Chem. Res.*, 2018, **51**, 619-627.

14. G. J. Zhou, M. Z. Li, J. Zhao, M. S. Molokeev and Z. G. Xia, *Adv. Opt. Mat.*, 2019, **7**, 1901335.

15. S. R. Li, J. J. Luo, J. Liu and J. Tang, *J. Phys. Chem. Lett.*, 2019, **10**, 1999-2007.

16. C. K. Zhou, H. R. Lin, M. Worku, J. Neu, Y. Zhou, Y. Tian, S. Lee, P. Djurovich, T. Siegrist and B. W. Ma, *J. Am. Chem. Soc.*, 2018, **140**, 13181-13184.

17. C. K. Zhou, H. R. Lin, J. Neu, Y. Zhou, M. Chaaban, S. Lee, M. Worku, B. H. Chen, R. Clark, W. H. Cheng, J. J. Guan, P. Djurovich, D. Z. Zhang, X. Lü, J. Bullock, C. Pak, M. Shatruk, M. H. Du, T. Siegrist and B. W. Ma, *ACS Energy. Letters.*, 2019, **4**, 1579-1583.

18. M. Z. Li, J. Zhou, G. J. Zhou, M. S. Molokeev, J. Zhao, V. Morad, M. V. Kovalenko and Z. G. Xia, *Angew. Chem.* , 2019, **58**, 18670-18675.

19. J. C. Yu, J. T. Kong, W. Hao, X. T. Guo, H. J. He, W. R. Leow, Z. Y. Liu, P. Q. Cai, G. D. Qian, S. Z. Li, X. Y. Chen and X. D. Chen, *Adv. Mater.*, 2019, **31**, e1806385.

20. J. H. Li, Z. F. Tan, M. C. Hu, C. Chen, J. J. Luo, S. R. Li, L. Gao, Z. W. Xiao, G. D. Niu and J. Tang, *Front. Optoelectron.*, 2019, DOI: 10.1007/s12200-019-0907-4.

21. Y. Y. Jing, Y. Liu, J. Zhao and Z. G. Xia, *J. Phys. Chem. Lett.*, 2019, DOI: 10.1021/acs.jpclett.9b03035, 7439-7444.

22. E. Oomen and G. J. M. R. B. Dirksen, *Mater. Res. Bullt.*, 1985, **20**, 453-457.

23. E. Oomen, W. Smit and G. J. J. o. P. C. S. S. P. Blasse, *J. Phys. C.*, 1986, **19**, 3263.

24. C. K. Zhou, H. R. Lin, Y. Tian, Z. Yuan, R. Clark, B. Chen, L. J. van de Burgt, J. C. Wang, Y. Zhou, K. Hanson, Q. J. Meisner, J. Neu, T. Besara, T. Siegrist, E. Lambers, P. Djurovich and B. W. Ma, *Chem. Sci.*, 2018, **9**, 586-593.

25. G. M. Sheldrick, *Acta Crystallogr A*, 2008, **64**, 112-122.

26. K. Brandenburg and M. J. G. S. Berndt, 2004.

27. V. J. T. i. n. c. r. f. t. r. TOPAS, 2002.

28. R. Reisfeld, L. Boehm and B. J. J. o. S. S. C. Barnett, 1975, **15**, 140-150.

29. E. Oomen, W. Smit and G. J. J. o. P. C. S. S. P. Blasse, 1986, **19**, 3263.

30. S. Li, Q. Hu, J. Luo, T. Jin, J. Liu, J. Li, Z. Tan, Y. Han, Z. Zheng and T. J. A. O. M. Zhai, 2019, **7**, 1901098.

31. Z. F. Tan, J. H. Li, C. Zhang, Z. Li, Q. S. Hu, Z. W. Xiao, T. Kamiya, H. Hosono, G. D. Niu, E. Lifshitz, Y. B. Cheng and J. Tang, *Adv. Funct. Mater.*, 2018, **28**, 1801131.

Supporting Information

Tunable photoluminescence in Sb³⁺-doped zero-dimensional hybrid metal halides with intrinsic and extrinsic self-trapped excitons

Jun Zhou[†], Mingze Li[‡], Maxim S. Molokeev[§, ⊥, Δ], Jiayue Sun[†], Denghui Xu[*,†], and Zhiguo Xia[*,‡,◊]

[†] School of Science, Beijing Technology and Business University, Beijing 100048, P. R. China

[‡] The Beijing Municipal Key Laboratory of New Energy Materials and Technologies, School of Materials Sciences and Engineering, University of Science and Technology Beijing, Beijing, 100083, China

[§] Laboratory of Crystal Physics, Kirensky Institute of Physics, Federal Research Center KSC SB RAS, Krasnoyarsk 660036, Russia

[⊥] Siberian Federal University, Krasnoyarsk, 660041, Russia

[Δ] Department of Physics, Far Eastern State Transport University, Khabarovsk, 680021, Russia

[◊] State Key Laboratory of Luminescent Materials and Devices and Institute of Optical Communication Materials, South China University of Technology, Guangzhou, 510641, China

Corresponding Author

*xiazg@scut.edu.cn
*xudh@btbu.edu.cn
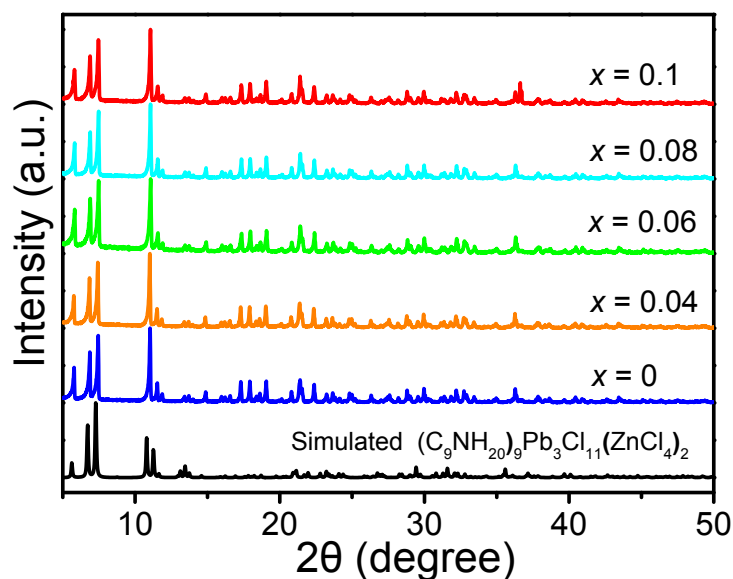
Fig. S1. The simulated and experimental X-ray powder patterns of $(C_9NH_{20})_9[Pb_3Cl_{11}](ZnCl_4)_2:Sb^{3+}$ with different Sb^{3+} contents.

Table S1. The crystal structure parameters of $(C_9NH_{20})_9[Pb_3Cl_{11}](ZnCl_4)_2$.

Formula moiety	$(C_9NH_{20})_9[Pb_3Cl_{11}](ZnCl_4)_2$
Molecular weight	2670.74
Temperature (K)	296
Space group, Z	$P31c$, 2
a (Å)	14.8386 (0)
c (Å)	30.6974 (13)
V (Å^3)	5853.5331 (6)
ρcalc (g/cm^3)	1.441
2_{max} (°)	46.4
R1 [$F_o > 4\sigma(F_o)$]	0.0735
$wR2$	0.231
$Goof$	1.116

S2

References

(1)   Sheldrick, G. M., A short history of SHELX. *Acta Crystallogr A* **2008,** *64* (Pt 1), 112-22.
(2)   Brandenburg, K.; Berndt, M. J. G. S., DIAMOND: Visual Crystal Structure Information System CRUSTAL IMPACT, Postfach 1251, D-53002 Boon. **2004**.
(3)   TOPAS, V. J. T. i. n. c. r. f. t. r., 2: General profile and structure analysis software for powder diffraction data–User's Manual; Bruker AXS: Karlsruhe, Germany. 2008. **2002**.